# Base Selectivity Is Impaired by Mutants that Perturb Hydrogen Bonding Networks in the RB69 DNA Polymerase Active Site†

Guangwei Yang, Jimin Wang, and William Konigsberg*

*Department of Molecular Biophysics and Biochemistry, Yale University, 333 Cedar Street, New Haven, Connecticut 06520*

*Received September 24, 2004; Revised Manuscript Received December 15, 2004*

ABSTRACT: To investigate the molecular basis for the selective utilization of nucleoside triphosphates complementary to templating bases, by RB69 DNA polymerase (RB69 pol), we constructed a set of mutants that we predicted would perturb the "floor" of the nascent base-pairing interface in the enzyme. We then determined the pre-steady-state kinetic parameters for the incorporation of complementary and noncomplementary dNTPs by the exo$^-$ form of RB69 pol and its mutants. We found that the Y567A mutant had the same $K_d$ and $k_{pol}$ values for incorporation of C versus G as the wild-type exo$^-$ enzyme; however, the $k_{pol}/K_d$ ratio for G versus G incorporation with the Y567A mutant was 10 times higher than the $k_{pol}/K_d$ efficiency of G versus G incorporation using the exo$^-$ RB69 pol. The reduced level of discrimination by the Y567A mutant against incorporation of mismatched bases was also seen with the Y391A mutant. Stopped-flow fluorescence was also employed to monitor rates of putative conformational changes with the exo$^-$ RB69 pol and its mutants using a primer−template complex containing 2-aminopurine. The rates of fluorescence changes were equal to or greater than the rates of the rapid chemical quench, indicating that we were monitoring a process occurring before or during the phosphoryl transfer reaction. We have interpreted our results within the context of the crystal structure of the RB69 pol ternary complex [Franklin, M. C., et al. (2001) *Cell 105*, 657−667].

DNA polymerases represent the central component of a multiprotein replicase responsible for ensuring faithful transmission of genetic information from parent to progeny. They do this by catalyzing a nucleotidyl transfer reaction that extends each nascent strand of the double-stranded DNA genome. In addition to their role in DNA replication, different members of the extensive DNA polymerase family also function in DNA repair and recombination (*2*).

One of the ongoing, unsolved problems is how DNA polymerases manage to replicate their genomes with such precision so that, in most organisms, only one mismatched base is incorporated for every $10^6$ bases copied (*3*−*5*). Several strategies that allow an organism to achieve this remarkably low error rate have been identified, each contributing to the overall fidelity of replication. Among these, the most important are base selection, editing by the polymerase, and base excision repair, a coordinated series of enzymatic reactions that come into play when a noncomplementary base is incorporated into a nascent DNA strand (*6*−*14*).

Enormous strides have been made in clarifying some aspects of base selection by DNA polymerases, but there is still much to be learned about mechanisms that allow DNA polymerases to discriminate among the four dNTP substrates. One way of approaching this problem is to determine the effect on base selection when amino acid substitutions are introduced in or near the nucleotide binding pocket of the polymerase. The impaired ability of these altered polymerases to discriminate among complementary and noncomplementary bases, in different combinations, should provide clues about how selectivity is achieved. The structural features of DNA polymerases that restrict base selection can be best understood if crystal structures of the wild-type polymerase, complexed with a primer−template complex (P/T)[1] and an incoming dNTP, as well as polymerase mutants, that affect base discrimination, are determined at high resolution. However, few examples of the desired complexes, especially those with mispaired bases, have been determined by X-ray crystallography, a notable exception being complexes of Bst1 DNA pol, a member of the A family of DNA polymerases (*15*).

DNA polymerases from T even bacteriophages such as T4 and RB69 belong to the B family and have several highly conserved sequence motifs that are found in all replicative B family DNA polymerases derived from eukaryotes (*16*−*18*). We have been studying structure−function relationships of RB69 pol, because of the abundance of genetic, structural, and kinetic data that has been obtained for this enzyme and for its close relative, T4 DNA polymerase (*1*, *19*−*31*).

In this paper, we report results obtained with an exo$^-$ derivative of RB69 pol (which we call the parental enzyme) and several of its pol active site mutants, with respect to

† This work was supported by U.S. Public Health Service Grants GM63276-01 to W. Konigsberg and GM57510 to T. A. Steitz.

* To whom correspondence should be addressed. Telephone: (203) 785-4599. Fax: (203) 785-7979. E-mail: william.konigsberg@yale.edu.

[1] Abbreviations: 2AP, 2-aminopurine; P/T, primer−template complex; ddP/T, dideoxy primer−template complex; RB69 pol, RB69 DNA polymerase; Ni−NTA, nickel−nitrilotriacetic acid; dFTP, 2,4-difluorotoluene deoxynucleoside triphosphate; dFMP, 2,4-difluorotoluene deoxynucleoside monophosphate.

10.1021/bi047921x CCC: $30.25 
Published on Web 02/11/2005

Table 1: Oligonucleotides Used To Prepare P/Ts for Kinetic Studies

| Primer /template | Nucleotide Sequence[a] | dNTP substrates used for assays |
|---|---|---|
| 13/20GT | 5′-CCGACCAGCCTTG<br>3′-GGCTGGTCGGAAC**G**TTTTTT | dCTP, dGTP |
| 13/20AC | 5′-CCGACCACGGAAC<br>3′-GGCTGGTGCCTTG**A**CCCCCC | dTTP, dFTP |
| 13/20A$_p$C | 5′-TCGCAGCCGTCCA<br>3′-AGCGTCGGCAGGT**A**$_p$CCCAAA | dTTP, dFTP |
| 12/20TA$_p$ | 5′-TCGCAGCCGTCC<br>3′-AGCGTCGGCAGGT**A**$_p$CCCAAA | dATP, |

[a] The nucleotide residues in boldface either are complementary to the incoming dNTPs or highlight the position of 2AP ($A_p$).

Table 2: Pre-Steady-State Kinetic Parameters for Utilization of dCTP and dGTP by the Parental RB69 DNA Polymerase and Its Mutants

| | dCTP/dG | | | dGTP/dG | | | |
|---|---|---|---|---|---|---|---|
| enzyme | $K_d$ ($\mu$M) | $k_{pol}$ ($s^{-1}$) | $k_{pol}/K_d$ ($\mu M^{-1}$ $s^{-1}$) | $K_d$ ($\mu$M) | $k_{pol}$ ($s^{-1}$) | $k_{pol}/K_d$ ($\mu M^{-1}$ $s^{-1}$) | selectivity[a] |
| parental | $69 \pm 16$ | $200 \pm 13$ | 2.9 | $(9.5 \pm 1.6) \times 10^3$ | $0.1 \pm 0.02$ | $1.1 \times 10^{-5}$ | $2.7 \times 10^5$ |
| Y567A | $68 \pm 4$ | $213 \pm 5$ | 3.1 | $210 \pm 32$ | $0.02 \pm 0.007$ | $9.5 \times 10^{-5}$ | $3.3 \times 10^4$ |
| Y567F | $(2.4 \pm 1.3) \times 10^3$ | $7.5 \pm 3.1$ | $3.1 \times 10^{-3}$ | NA[b] | NA[b] | NA[b] | NA[b] |
| Y391A | $980 \pm 200$ | $155 \pm 30$ | 0.16 | $750 \pm 350$ | $(5.8 \pm 1.1) \times 10^{-3}$ | $7.7 \times 10^{-6}$ | $2.0 \times 10^4$ |
| Y391F | $90 \pm 4$ | $312 \pm 4$ | 3.5 | $(5.3 \pm 2.0) \times 10^3$ | $0.08 \pm 0.02$ | $1.5 \times 10^{-5}$ | $2.3 \times 10^5$ |
| T587A | $220 \pm 60$ | $50 \pm 4$ | 0.23 | NA[b] | NA[b] | NA[b] | NA[b] |
| T587A/Y391A | $(1.7 \pm 0.7) \times 10^3$ | $54 \pm 12$ | $3.2 \times 10^{-2}$ | NA[b] | NA[b] | NA[b] | NA[b] |
| T587A/Y391F | $660 \pm 180$ | $210 \pm 22$ | 0.32 | NA[b] | NA[b] | NA[b] | NA[b] |

[a] The selectivity for dCTP over dGTP is given by the ratio of $k_{pol}/K_d$ for dCTP utilization divided by $k_{pol}/K_d$ for dGTP utilization. [b] The kinetic parameters could not be measured due to either the very high $K_d$ values (>10 mM) or the very low $k_{pol}$ values (<0.01 $s^{-1}$).

their ability to incorporate dGMP opposite a templating G compared to incorporating dCMP opposite a templating G. We have determined the relevant pre-steady-state kinetic parameters using rapid chemical-quench and stopped-flow fluorescence in an attempt to estimate rates of conformational changes when the parental enzyme and its mutants are converted from a binary to a ternary complex poised for the phosphoryl transfer reaction. The kinetic parameters for other mispaired bases using these RB69 pol mutants are being determined and will be reported subsequently.

## MATERIALS AND METHODS

T4 polynucleotide kinase was obtained from New England Biolabs and [$\gamma$-$^{32}$P]ATP from Perkin-Elmer Life Sciences Inc. dNTPs and dCTP$\alpha$S were obtained from Amersham/Pharmacia and electrophoresis reagents from American Bioanalytical Corp. 2′,4′-Difluorotoluene deoxynucleoside 5′-triphosphate (dFTP) was kindly provided by E. Kool (Stanford University, Palo Alto, CA). Oligonucleotides (Table 1) were provided by the W. M. Keck Foundation Biotechnology Resource Laboratory (Yale University). All other chemicals were analytical grade. The RB69 pol derivatives used in this study carry the D222A/D327A double mutation that eliminates 3′−5′ exonuclease activity.

*Construction and Preparation of Mutants.* Plasmid pCW50 harboring cDNA for the exonuclease deficient form of RB69 pol (D222A/D327A) was subjected to site-directed mutagenesis to introduce Ala or Phe for the residues listed in Table 2 using the PCR-based protocol of the Quikchange site-directed mutagenesis kit (Stratagene). The presence of the desired altered codons and the absence of other spurious changes in the cDNA coding insert were confirmed by DNA sequencing. Expression and purification of the mutant RB69 pols were carried out as previously described (*29*) with the following modification. Since there were six His residues appended to the C-terminus of the expressed polymerases mutants, we used a Ni−NTA column for the initial purification followed by a cleanup step on a Source 30Q column (*29*). The purity of the RB69 pol mutant preparations was estimated by SDS−PAGE and the enzyme concentrations determined spectrophotometrically as previously described (*30*).

*Pre-Steady-State Burst and Single-Turnover Experiments.* Pre-steady-state rapid chemical quench experiments were performed using the KinTek Quench-Flow Instrument (model RQF-3, Kintek Corp., University Park, PA). For slower reactions, requiring sampling at time intervals of >20 s, aliquots were removed manually and quenched with 0.5 M EDTA. Unless otherwise noted, all components of the reactions are reported as final concentrations after mixing. Burst assays were performed under conditions where the P/T concentration was 3 times greater than that of the enzyme and using l mM dCTP, a concentration well above saturation. Reactions were carried out at 25 °C by mixing equal volumes of 66 mM Tris-HCl (pH 7.5) containing the preincubated complex of 2 $\mu$M 5′-$^{32}$P-labeled primer-template and 600 nM RB69 pol (either the parental enzyme or its mutants) with 66 mM Tris-HCl (pH 7.5) containing 20 mM $MgSO_4$ and 2 mM dCTP. The final concentrations were 1 $\mu$M P/T, 300 nM enzyme, and 1 mM dCTP. The polymerization reaction was quenched with 0.5 M EDTA at defined time intervals. Products were analyzed by gel electrophoresis (20% polyacrylamide−50% urea) and quantified by gel scanning using a phosphorimager (Molecular Dynamics). Single-turnover assays were performed in a manner similar to that described above except that 2 $\mu$M enzyme was used, a concentration 6.7 times higher than the concentration of the P/T (300 nM). The concentrations of dNTPs were varied to

determine $K_d$ and $k_{pol}$ values. The sequences of the P/T for primer extension assays are given in Table 1.

*Stopped-Flow Fluorescence.* Stopped-flow experiments were performed with an Applied Photophysics stopped-flow spectrofluorometer (SX.18MV). The excitation wavelength was 313 nm, and emission was monitored by using a 335 nm cutoff filter. Reactions were performed under single-turnover conditions in a manner similar to the rapid chemical-quench assay with final concentrations of 2 $\mu$M enzyme, 300 nM P/T, and 80 $\mu$M dTTP or either dATP or dFTP depending on the template. The P/T substrates containing 2AP in the template strand used for monitoring fluorescence changes are given in Table 1.

*Data Analysis.* Data from burst assays were fit to the burst equation [product] = $A[1 - \exp(k_{ob}t)] + k_{ss}t$, where $A$ represents the amplitude of the burst which provides an estimate of the concentration of enzyme active sites, $k_{ob}$ is the observed first-order rate constant for dNTP incorporation, and $k_{ss}$ is the observed steady-state rate constant.

Data from single-turnover experiments were fit to the equation for a single exponential. The dissociation constant, $K_d$, for dNTP binding to the RB69 pol−13/20mer (E−P/T) complex was calculated by fitting data to the equation $k_{obs} = (k_{pol}[S])/(K_d + [S])$, where $k_{pol}$ is the maximum rate of dNTP incorporation, [S] is the concentration of incoming dNTP, and $K_d$ is the dissociation constant for the incoming dNTP in the E−P/T−dNTP complex.

## RESULTS

The main objective of this study was to achieve a better understanding of how several conserved residues in RB69 pol influence base selection and to determine how replacement of these residues affects the binding affinity and reaction rate for correctly matched versus mispaired dNTPs during primer extension. For this purpose, we constructed a set of mutant RB69 pols, choosing residues for substitution that appeared to be part of the nucleotide binding pocket as well as residues that had hydrogen bonding or van der Waals interactions with side chains of residues in the active site (*1*). Accordingly, residues Y567, Y391, and T587 were replaced with Ala or Phe. We also prepared two double mutants (combinations of the replacements mentioned above) to see if base discrimination was further reduced. The locations of these residues with respect to the primer−template terminus and the incoming dNTP are shown in Figure 1A. The space filling (CPK) image of this region (Figure 1B) illustrates the close packing of these residues stabilized in part by van der Waals interactions. We then performed rapid chemical quench experiments to determine $K_d$ and $k_{pol}$ values for incorporation of correct and mispaired dNMPs to evaluate the relative contributions of binding affinity and rates of dNMP incorporation to base selectivity. Stopped-flow fluorescence experiments were also carried out with 2-aminopurine (2AP) in the template strand to provide an independent means of estimating rates of change in the environment surrounding the 2AP residues (stacking or unstacking with adjacent bases).

*Burst Assays.* Burst experiments showed a biphasic rate for product formation with the parental enzyme as well as with the Y567A mutant, indicating that a step following chemistry was rate-limiting (Figure 2). The concentration

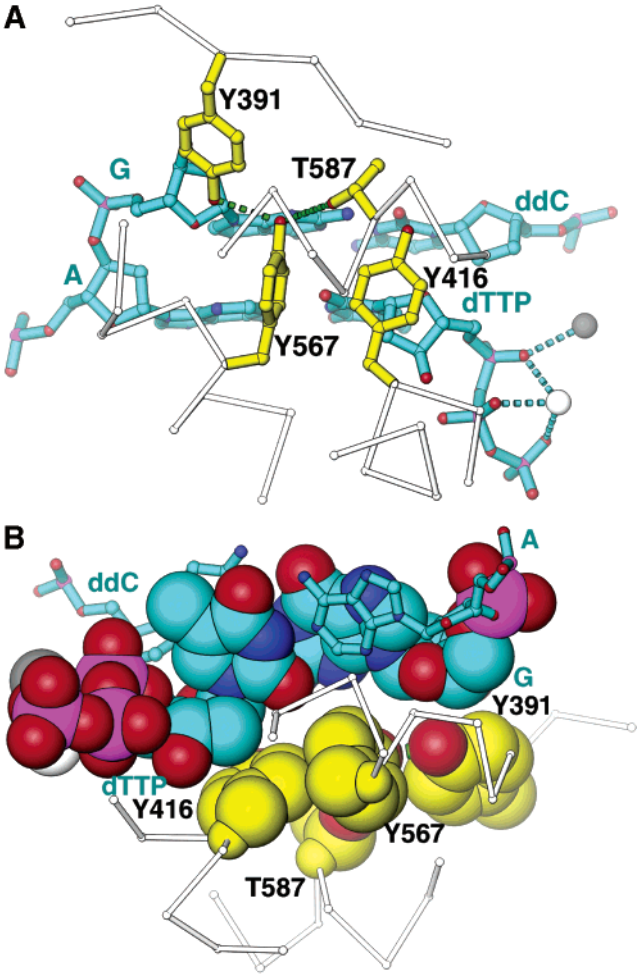


FIGURE 1: Selected active site residues in the ternary complex of RB69 DNA polymerases. (A) Location of the four residues (yellow) that comprise the "floor" of the nascent base pair platform in the RB69 pol ternary complex. The figure also includes the position of the ddP/T with the incoming dTTP opposite the templating A (all in blue). The A and B metal ions are shown in gray and white, respectively. Parts of the Cα trace (thin white bars) are also included. Hydrogen bonds are represented by dashed green cylinders. The figure is based on the data of Franklin et al. (*1*) (PDB entry 1IG9) except that the most energetically favorable rotamer position of the T587 side chain was used as observed in the binary RB69 pol−P/T complex (*23*). (B) Space filling representation of the selected active site residues used in this study showing that Y416 makes van der Waals contacts with the ribose of incoming dTTP and Y391 contacts the ribose of the second template nucleotide G that is base paired with ddC. Y567 is in contact with both base pairs near the center of the minor groove.

of the productively bound form of the P/T in the E−P/T complex was determined from the amplitude of the burst and found to be 71% for the Y567A mutant. No burst with the Y567F mutant suggests that chemistry or steps before chemistry were rate-limiting (data not shown).

*Pre-Steady-State Kinetic Parameters for Incorporation of Complementary dNMPs by the Parental Enzyme and Its Mutants.* To determine the $K_d$ values for incoming dNTPs and the maximum rate ($k_{pol}$) for the nucleotidyl transfer reaction with the parental enzyme as well as with the Y567A and Y567F mutants, we varied dNTP concentrations under single-turnover conditions. For the correctly matched incoming dCTP, the Y567A mutant had the same $K_d$ and $k_{pol}$ values as the parental enzyme (Figure 3A and Table 2), whereas

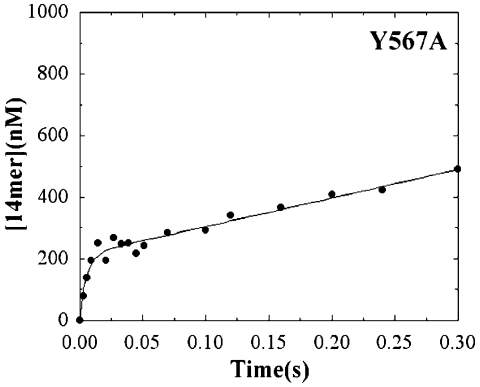


FIGURE 2: Burst assay for the Y567A mutant of RB69 pol. 13/20GT (2 $\mu$M) was preincubated with the Y567A mutant (600 nM) in 66 mM Tris-HCl (pH 7.5) and then mixed with an equal volume of 2 mM dCTP and 20 mM $Mg^{2+}$ in 66 mM Tris-HCl (pH 7.5) from the second syringe to start the reaction. The final concentrations were 1 $\mu$M P/T, 300 nM enzyme, 1 mM dCTP, and 10 mM $Mg^{2+}$. The reactions were quenched at the indicated times and analyzed after urea−acrylamide gel electrophoresis by phosphorimaging. The solid line represents the best fit to the burst equation as described in Materials and Methods. The amplitude *A* was 212 ± 9 nM; the burst rate $k_{ob}$ was 185 ± 35 $s^{-1}$, and the steady-state rate $k_{ss}$ was 4.4 ± 0.3 $s^{-1}$.

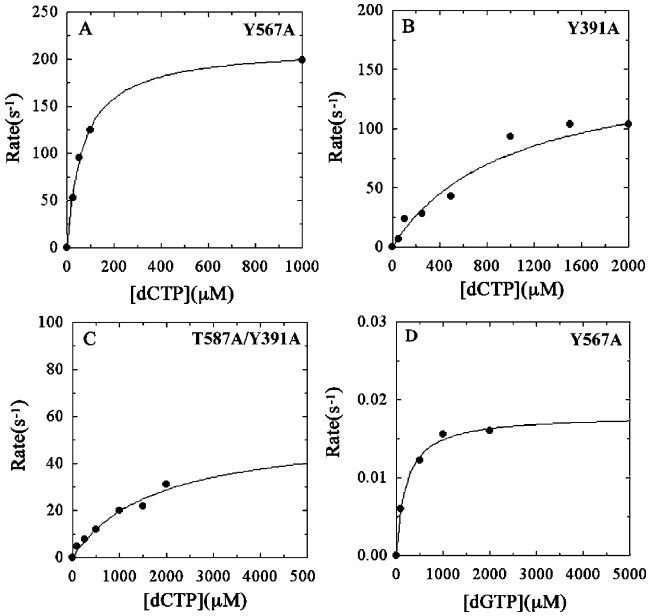


FIGURE 3: dCTP and dGTP concentration dependence of the observed rate constants for primer extension by RB69 pol mutants. The pre-steady-state rates were plotted against the dCTP or dGTP concentration and fit to the hyperbolic equation for $K_d$ determination as described in Materials and Methods: (A) Y567A, (B) Y391A, (C) T587A/Y391A, and (D) dGTP vs templating G with the Y567A mutant. The $K_d$ and $k_{pol}$ values determined from the graphs for the various mutants are presented in Table 2.

the Y567F mutant showed a dramatic increase in $K_d$ and a large decrease in $k_{pol}$ (Table 2).

To further investigate the role of Y567 in base selection, two other residues, Y391 and T587, which can potentially form *direct* hydrogen bonds with the $\gamma$-hydroxyl group of Y567 (*1*), were replaced with either A or F and the resulting RB69 pol mutants studied by rapid chemical quench techniques. For correct dCMP incorporation, the Y391F mutant had kinetic parameters similar to those of the parental enzyme, while the Y391A mutant had a 14-fold higher $K_d$ but a $k_{pol}$ that was nearly the same as that of the parental enzyme (Table 2).

Two double mutants, T587A/Y391A and T587A/Y391F, were also investigated using complementary incoming dNTPs. T587A/Y391A exhibited a 25-fold higher $K_d$ and a 4-fold lower $k_{pol}$ relative to those of the parental enzyme, while the T587A/Y391F mutant exhibited a 10-fold higher $K_d$ and an identical $k_{pol}$ compared to those of the parental enzyme (Figure 3C and Table 2).

*Pre-Steady-State Kinetic Parameters for Incorporation of Noncomplementary dNMPs by the Parental Enzyme and by the Y567A and Y567F Mutants*. After determining the kinetic parameters for correct dNMP incorporation, we then examined the kinetics of dGMP incorporation using a 13/20GTmer P/T so that dGTP was paired with a templating G. Using the parental enzyme, the Y567A and Y567F mutants, we compared the $k_{pol}/K_d$ ratio for incorporation of the correctly paired dCMP with the $k_{pol}/K_d$ ratio found for the G versus G mispair. The parental enzyme had a much higher $K_d$ and a greatly reduced $k_{pol}$ for the incorporation of mispaired dGMP relative to those of the correctly paired dCMP (Figure 3D and Table 2). The Y567A mutant had a 50-fold lower $K_d$ and a 5-fold lower $k_{pol}$ for incorporation of dGMP versus G compared to those of the parental enzyme; therefore, the overall selectivity was 10 times lower for the Y567A mutant than for the parental enzyme (Table 2). The kinetic parameters for dGMP versus G incorporation by the Y567F mutant could not be determined because of the very high $K_d$ and/or the very low $k_{pol}$.

Another approach was employed to determine the roles of hydrogen bonds involving the $\gamma$-hydroxyl group of Y567 for utilization of the noncomplementary dGTPs. In these experiments, all hydrogen bonding partners of the Y567 $\gamma$-hydroxyl group had their side chains replaced with methyl groups (i.e., the T587A/Y391A double mutant), while the Y567 $\gamma$-hydroxyl group itself was removed in the Y567F mutant. Unfortunately, kinetic parameters for incorporation of dGMP opposite G could not be determined for the T587A/Y391A double mutant, since the $K_d$ and $k_{pol}$ values were beyond the range that could be measured experimentally.

*Pre-Steady-State Kinetic Parameters for dFMP Incorporation by the Parental Enzyme and the Y567A and Y567F Mutants*. Since it is apparent that the Y567A mutant can utilize mispaired bases more efficiently than the parental enzyme, it was of interest to determine whether a triphosphate of a nucleoside base analogue, 2,4-difluorotoluene (F), which is isosteric with T, would be utilized with the same efficiency as dTTP. Since the kinetics of dFMP incorporation has been studied only under steady-state conditions with KF and T7 DNA pol (*32*, *33*), we decided to determine the pre-steady-state kinetic parameters for dFMP incorporation with the parental RB69 pol and with the Y567A mutant. This allowed us to compare ground state binding affinities and the maximum rates of phosphoryl transfer with dFTP and dTTP using the parental and Y567A mutant pols. The results showed that the parental enzyme and the Y567A mutant had slightly higher $K_d$ values (5−13-fold) and much lower (more than 100-fold) $k_{pol}$ values for dFMP relative to dTMP incorporation. Thus, the selectivity factor for dTTP versus dFTP was ~1000 with both the parental enzyme and the Y567A mutant (Table 3). There was no detectable dFMP incorporation by the Y567F mutant even with high concen-

Table 3: Pre-Steady-State Kinetic Parameters for Utilization of dTTP and dFTP by the Parental RB69 DNA Polymerase and the Y567A Mutant

| | dTTP | | | dFTP | | | |
|---|---|---|---|---|---|---|---|
| enzyme | $K_d$ ($\mu$M) | $k_{pol}$ ($s^{-1}$) | $k_{pol}/K_d$ ($\mu M^{-1}$ $s^{-1}$) | $K_d$ ($\mu$M) | $k_{pol}$ ($s^{-1}$) | $k_{pol}/K_d$ ($\mu M^{-1}$ $s^{-1}$) | selectivity[a] |
| parental | $51 \pm 10$ | $273 \pm 16$ | 5.4 | $268 \pm 27$ | $1.8 \pm 0.1$ | $6.7 \times 10^{-3}$ | 790 |
| Y567A | $33 \pm 2$ | $301 \pm 6$ | 9.1 | $418 \pm 87$ | $2.7 \pm 0.3$ | $6.5 \times 10^{-3}$ | $1.4 \times 10^3$ |

[a] The selectivity for dTTP over dFTP is given by the ratio of $k_{pol}/K_d$ for dTTP utilization divided by $k_{pol}/K_d$ for dFTP utilization.

trations of dFTP (2 mM) and long incubation times (1 h).

*Stopped-Flow Fluorescence*. To further investigate the role of Y567 in base selection, stopped-flow fluorescence experiments were carried out to monitor the rates of change in the environment surrounding the 2AP residues during nucleotide incorporation with the parental enzyme and with the Y567A and Y567F mutants. For this purpose, 2AP was placed at two different positions in the template strand: as the templating base in the *n* position (opposite to the incoming dNTP) or at the adjacent position ($n + 1$) just 5′ to the templating base (Table 1). When 2AP was in the *n* position, both the parental enzyme−P/T complex and the Y567A−P/T complex exhibited biphasic kinetics that best fit a double exponential as shown by the stopped-flow fluorescence data for dTMP incorporation under single-turnover conditions (Figure 4A). The rates for the two phases were 176 and 16 $s^{-1}$, respectively, for the parental enzyme (WT) using 80 $\mu$M dTTP (Table 4) and 254 and 8 $s^{-1}$, respectively, for the Y567A mutant (Figure 4B). In contrast, the data for the Y567F mutant best fit a single exponential with a rate of 0.17 $s^{-1}$ (Figure 4C). These stopped-flow fluorescence results are generally consistent with the rapid chemical quench experiments described above. For example, the rate for the fast phase with the parental enzyme (176 $s^{-1}$, Table 4) is similar to the rate (154 $s^{-1}$, Table 4) for dTMP incorporation determined by rapid chemical quench experiments. The rate of fluorescence quenching for the Y567A mutant (254 $s^{-1}$) is only 1.5 times greater than that observed for the parental enzyme. However, there are some other noticeable differences between the behavior of the two enzymes; for example, amplitude $A_1$ of the fast phase was much lower (0.1 V for the Y567A mutant vs 0.3 V for the parental enzyme as shown in Table 4). Whether these differences are due to the direct effect of the Y567A mutation on the fluorescence of 2AP or to other differences between the two enzymes that influence the rate of quenching is not known. Stopped-flow fluorescence also revealed a new slower phase exhibited by both the parental enzyme and the Y567A mutant that was not observed with rapid chemical quench techniques. This new, slower phase was not seen with the Y567F mutant.

The rates of change in fluorescence were not dependent on the location (*n* vs $n + 1$ position) of the 2AP probe with either the parental enzyme or the Y567A mutant. When 2AP was in the $n + 1$ position, the rates for the parental enzyme are 176 $s^{-1}$ for the fast phase (unchanged from rates with 2AP in the *n* position) and 39 $s^{-1}$ for the slow phase, a slight increase over the rate of 16 $s^{-1}$ found when 2AP was in the *n* position (Figure 4D). The rates for the Y567A mutant with 2AP in the $n + 1$ position were 269 $s^{-1}$ for the fast phase (unchanged from that at the *n* position) and 5 $s^{-1}$ for the slow phase (Figure 4E). This small variation in rate may be due to a difference in the way base stacking of 2AP is affected in the two sets of experiments. Similarly, the rate of fluorescence enhancement for the Y567F mutant with 2AP in the $n + 1$ position was also slow (0.18 $s^{-1}$), followed a single exponential, and was consistent with results from the rapid chemical quench experiments (Figure 4F and Table 4).

An attempt was also made to extend the stopped-flow fluorescence experiments to examine the effect of noncomplementary dNTPs and dFTP on 2AP fluorescence. No detectable change in 2AP fluorescence was observed with either the parental enzyme or any of the Y567 mutants when noncomplementary dNTPs were added to the enzyme−P/T complex (data not shown). With dFTP, only the parental enzyme exhibited changes in the stopped-flow fluorescence with a rate of 0.08 $s^{-1}$ (Table 4). The rate of fluorescence quenching also fit best to a single exponential and was consistent with the results of the rapid chemical quench experiments (0.07 $s^{-1}$) shown in Table 4.

## DISCUSSION

*Residue Y567 Is Involved in Base Selection*. We have attempted to interpret pre-steady-state kinetic parameters for primer extension with correct (C vs G) and incorrect (G vs G) base pairs in terms of structural features of RB69 pol and several of its single-site mutants. From our previous work, we knew that Y567 had a role in base discrimination (*34*), but it was unclear whether other residues, which appeared to interact with Y567 via a hydrogen bonding network (Figure 1A), were also able to influence base selection. To address this issue, we substituted Ala for Tyr at residue 567, and in separate experiments, we replaced Y391 and T587 with Ala. We also constructed and tested the Y391A/T587A and Y391F/T587A double mutants for their ability to incorporate complementary and noncomplementary dNMPs. The Ala for Tyr replacement at residue 567 had no effect on the pre-steady-state kinetic parameters for incorporation of dNMPs that were correctly paired with templating bases. However, since the Y567A mutant was able to utilize dGTP opposite a G more efficiently than the parental enzyme, it is clear that Y567 places constraints on base selection (Table 2). We offer an explanation for this loss of selectivity based on (i) the crystal structure of the ternary complex of the parental enzyme with a dideoxy P/T and a complementary dNTP (*1*), (ii) the structure of a G·G mismatch in a DNA duplex in the absence of any proteins (*35*), and (iii) docking of this G·G mismatch into the observed ternary complex using the parental enzyme and the computer-generated structure of the Y567 mutants. In the crystal structure of the ternary complex (*1*), the phenyl ring of Y567 favors correct versus incorrect Watson−Crick base pairing for the nascent base pair as the rotamer conformation of the Y567 side chain is restricted because of a hydrogen bonding network that includes the hydroxyl groups of Y391

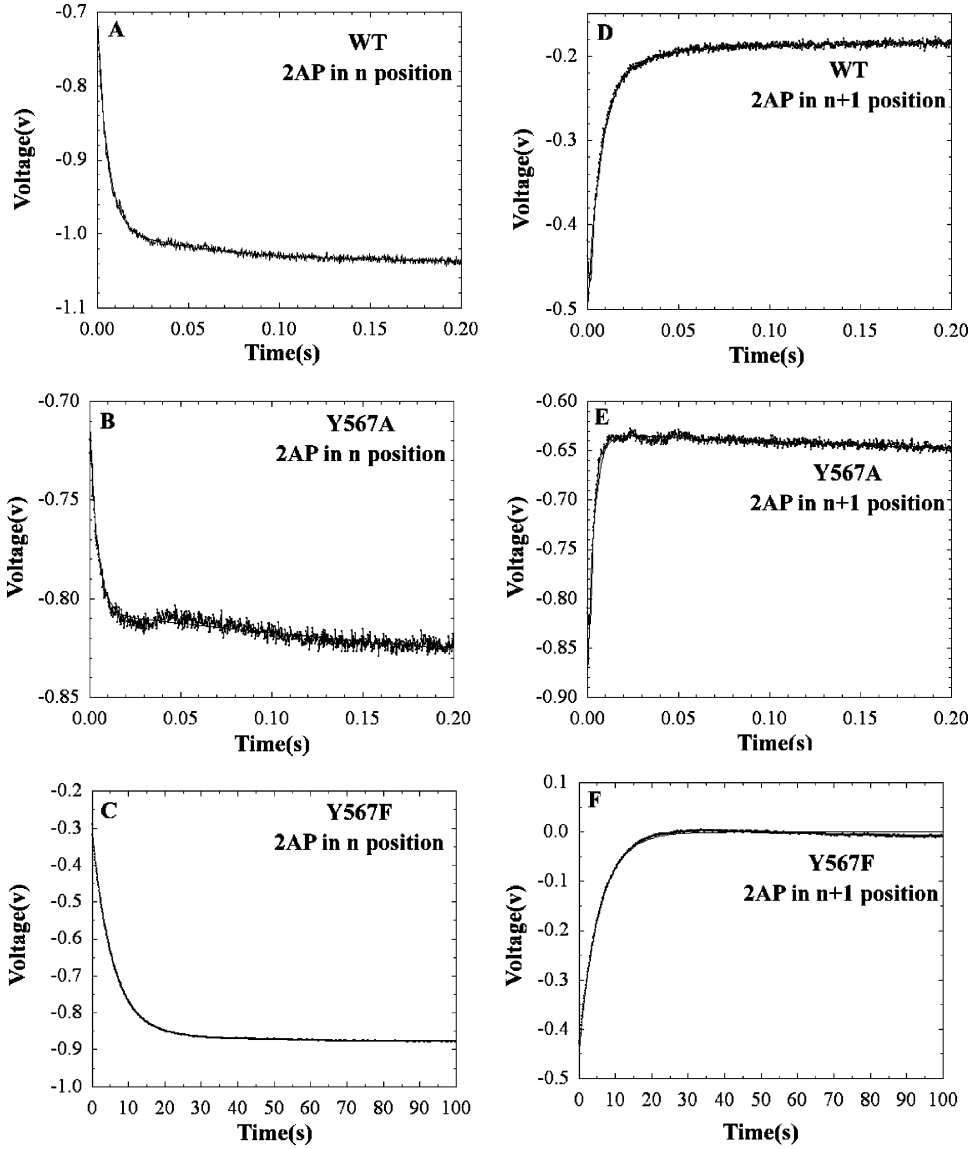


FIGURE 4: Stopped-flow fluorescence assay for primer extension with the 13/20$A_p$Cmer or the 12/20$TA_p$mer. Measurements and data analysis were performed as described in Materials and Methods. In general, excess RB69 pol or its mutants were preincubated with 600 nM 13/20$A_p$Cmer or 12/20$TA_p$mer in syringe A. Reactions were initiated by mixing the contents of syringe A with an equal volume of the solution from syringe B that contained 160 $\mu$M dTTP (for the13/20$A_p$Cmer) or 160 $\mu$M dATP (for the 12/20$TA_p$mer) and 20 mM $Mg^{2+}$. The rates and amplitudes for the fluorescence changes are summarized in Table 4. (A) Incorporation of dTMP into the 13/20$A_p$Cmer by the parental enzyme. (B) Incorporation of dTMP into the 13/20$A_p$Cmer by the Y567A mutant. (C) Incorporation of dTMP into the 13/20$A_p$Cmer by the Y567F mutant. (D) Incorporation of dAMP into the12/20$TA_p$mer by the parental enzyme. (E) Incorporation of dAMP into the 12/20$TA_p$mer by the Y567A mutant. (F) Incorporation of dAMP into the 12/20$TA_p$mer by the Y567F mutant.

Table 4: Summary of Stopped-Flow Fluorescence Assays[a]

| | | | | | fluorescence change | | | | |
|---|---|---|---|---|---|---|---|---|---|
| primer/template | 2AP position | incoming dNTP | enzyme | up/down | $A_1$ (V) | $k_1$ ($s^{-1}$) | $A_2$ (V) | $k_2$ ($s^{-1}$) | primer extension rate ($s^{-1}$)[b] |
| 13/20$A_p$C | *n* | dTTP | parental | ↓ | 0.3 | 176 | 0.06 | 16 | 154 |
| | | | Y567A | ↓ | 0.1 | 254 | 0.02 | 8 | 167 |
| | | | Y567F | ↓ | 0.56 | 0.17 | NA | NA | 0.13 |
| 13/20$A_p$C | *n* | dFTP | parental | ↓ | 0.21 | 0.08 | NA | NA | 0.07 |
| | | | Y567A | no signal | NA | NA | NA | NA | 0.15 |
| | | | Y567F | no signal | NA | NA | NA | NA | NA |
| 12/20$TA_p$ | *n* + 1 | dATP | parental | ↑ | 0.3 | 176 | 0.07 | 39 | 102 |
| | | | Y567A | ↑ | 0.25 | 269 | 0.03 | 5 | 176 |
| | | | Y567F | ↑ | 0.44 | 0.18 | NA | NA | 0.16 |

[a] Precision: $A_1$, ±15%; $k_1$, ±20%; $A_2$, ±40%; $k_2$, ±20%. [b] Primer extension rates were obtained from chemical quench data and had a precision of ±20%.

and T587 (Figure 1A). Since the aromatic ring of Y567 forms part of the nascent base pair binding pocket, it limits the space that can be occupied on the minor groove side of the nascent base pair (*1*). By removal of the phenolic side chain

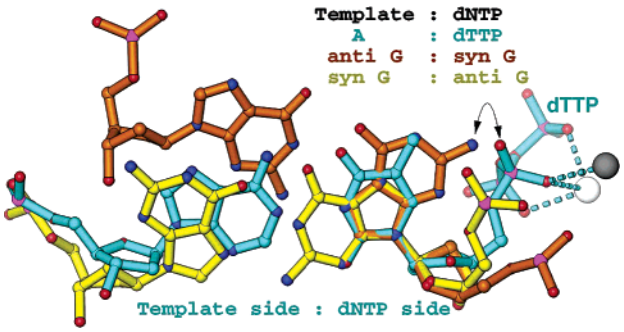


FIGURE 5: Modeling of the conformational forms of G·G mispairs based on the duplex DNA structure determined by Skelly et al. (*35*). In this model, the templating G and the incoming dGTP in the anti and syn conformations are colored brown. The syn templating G and the anti incoming G are colored yellow. Four atoms of each of these G·G conformers were superimposed onto the dTTP·A pair. Two of the atoms of the G·G conformers were from the glycosidic bond, and the other two atoms were from the base that connects to the glycosidic bond.

in the Y567A mutant, the polymerase is able to better accommodate the noncanonical base pairing of G versus G as evidenced by a 50-fold increase in the ground state binding affinity of the mutant relative to that of the parental enzyme (Table 2). Since this Y to A replacement does not interfere with the geometry of the correctly paired dCTP, it was reassuring that neither the affinity nor the incorporation rate of the correct dNTP was affected (Table 2). It seems reasonable therefore to propose that Y567, when restricted in its rotamer conformation, provides a steric gate for checking Watson−Crick base pairing. Unlike Y416, which is parallel to the ribose ring of the incoming dNTP, the phenyl ring of Y567 is perpendicular to both the templating base and to Y416 (Figure 1A,B). Moreover, the torsion angle of the Y567 C$\alpha$−C$\beta$ bond is 145°, which is its least favorable conformation as it lies midway between two other preferred rotamer positions. This unfavorable conformation is maintained via a hydrogen bonding network because there are few nonpolar interactions between Y567, Y416, and other residues in RB69 pol.

There is, however, an additional issue that has to be considered in interpreting the results, namely, the conformation of the incoming dGTP versus the templating G. On the basis of the crystal structure of oligonucleotide duplexes containing G·G base pairs (*35*), it seems that one G residue has to adopt the syn conformation while the other is required to be in the anti conformation. In the attempt to model a G·G mispair into the RB69 pol ternary structure, it becomes clear that only when the templating G is in the anti and the incoming G in the syn conformation can dGMP be incorporated into the primer strand. This is illustrated in Figure 5 in which four atoms of the two different conformations of the templating G and the mispaired dGTP are superimposed onto four atoms of a templating A and an incoming dTTP. The four atoms chosen include two from the glycosidic bond and two from bases that are connected to the glycosidic bonds. Only when these four atoms are superimposed can the $\gamma$-phosphate (as well as the remainder of the triphosphate tail) be positioned so that they correspond to the same location occupied by dTTP (when paired with A) in the ternary structure (*1*). Modeling demonstrates that dGTP can be correctly positioned only if it adopts the anti and not the syn conformation. If it were in the syn conformation, the exocyclic amino group of G would sterically clash with its own nonbridging $\alpha$-phosphate oxygen in the triphosphate tail of the incoming dGTP (as indicated by the arc with the double-headed arrow in Figure 5). Also, the templating G would deviate substantially from its expected position. If dGTP adopts the anti conformation, then both the templating G (syn) and the incoming G (anti) would be close to the positions expected for a nascent base pair (Figure 5). In the absence of both the enzyme and incoming dGTP, the G nucleotide at the templating position would most likely adopt the anti conformation for maximal stacking interactions within the DNA duplex. Therefore, upon the formation of a ternary complex with the enzyme and incoming dGTP, the templating G has to flip from the usual anti to the syn conformation. The flipping would seldom occur were it not for the polymerase being able to trap and incorporate the G·G mispair, albeit with low efficiency ($k_{pol}/K_d = 1 \times 10^{-5}$ $\mu M^{-1}$ $s^{-1}$). The efficiency of dGMP incorporation is markedly improved when Y567 is replaced with Ala ($k_{pol}/K_d = 9.5 \times 10^{-5}$ $\mu M^{-1}$ $s^{-1}$) in which more space is available in the polymerase binding pocket for flipping to occur (Table 2). The difference between the parental enzyme and the Y567A mutant in their ability to incorporate a G·G mispair can be attributed to the 50-fold decrease in $K_d$ for dGTP versus a templating G exhibited by the Y567A mutant compared to the parental enzyme. Note that the $k_{pol}$ for incorporating dGMP opposite G with the Y567A mutant is only 5 times less than that of the parental enzyme, indicating that there is a slightly less favorable geometry for the nascent base pair with respect to the primer terminus when the Y567A mutant is compared to the parental enzyme. Nevertheless, since the $k_{pol}$ for the G versus G pair is so drastically reduced for both the parental enzyme and the Y567A mutant, it would suggest that the geometry of the G·G nascent base pair, with respect to the attacking 3′-OH, must be markedly perturbed. This notion is clearly consistent with the modeling (Figure 5). A plausible reason for the $K_d$ difference is that there is more space in the nucleotide binding pocket with the Y567A mutant, making it easier for the templating base to flip from the anti to the syn configuration. The rigidly positioned Y567 in the parental enzyme presents a barrier to flipping which is then manifested in the higher $K_d$ exhibited by the parental enzyme for the G·G mispair. To summarize, it would appear that Y567 is optimally positioned to check for correct Watson−Crick base pairing since it establishes a geometrical constraint in the nucleotide binding pocket (Figure 6).

A remaining problem is how to account for the dramatically weakened ability of the Y567F mutant to extend a primer even with a dNTP that is complementary to the templating base. This result was unexpected because, with the $\gamma$-hydroxyl group absent in the Y567F mutant, the side chain of residue Y567 is free to assume a more favorable rotamer conformation which it presumably does to relax the strain. Surprisingly, in the modeled structure of the Y567F mutant ternary complex with a ddP/T and a complementary dNTP (structure not shown in this paper), the ddP/T is displaced from the position that it normally occupies in the parental enzyme. This displacement also distorts the nucleotide binding pocket, dramatically reducing the affinity of the incoming dNTP. Even when a correct, nascent base pair is formed, the position of the incoming dNTP relative to the

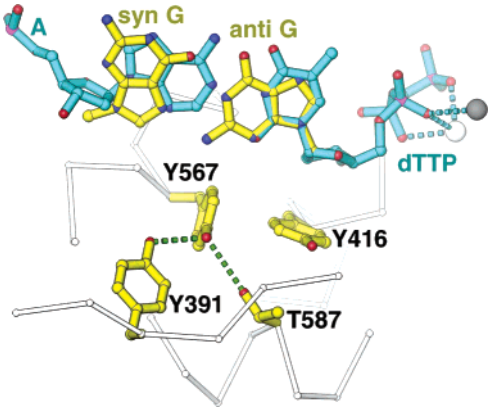


FIGURE 6: Modeling of the G·G mispair (yellow) vs the A·T pair (cyan) in the RB69 pol ternary complex. We assume that the G·G mispair in the polymerase adopts the same structure as without it (modeled in Figure 5). Only the anti conformation of dGTP is possible and depicted here, because in the syn conformation its base runs into the α-phosphate oxygen and its templating nucleotide on the opposite strand is substantially displaced from the observed location shown in Figure 5.

3′-OH of the primer is perturbed which would result in a severe misalignment between the attacking 3′-OH group and the α-phosphorus atom of the incoming dNTP. The distortion of the nucleotide binding pocket and the suboptimal geometry of the reactants in the active site can readily rationalize the failure of the Y567F mutant to catalyze the phosphoryl transfer reaction. A critical test of this rationalization will come from the crystal structure of this mutant complexed with a P/T and a dNTP, work that is being performed in C. Kisker's lab at the State University of New York, Stony Brook, NY (personal communication**)**.

The hydrogen bonding network that is crucial for restricting the Y567 rotamer conformation includes Y391 and potentially also T587 (Figure 1A). By examining the environment of the γ-hydroxyl group of Y567 in the apo-RB69 pol structure (*18*), we have identified a well-defined hydrogen bond that could be formed with Y391 and another potential hydrogen bond with T587 that may explain why the latter residue is also conserved. Currently, the side chain of T587 adopts its second most favorable rotamer conformation, in which its Cγ2 is within 3.2 Å of the γ-hydroxyl of Y567. If the most favored rotamer conformation is modeled, Oγ2 of T587 will be occupied by Oγ1 and a hydrogen bond will be formed with Y567 (Figure 1A). Modeling also suggests that such a choice is clearly possible in the apo-RB69 pol structure, but not in the ternary complex. Each of the single mutants, T587A and Y391A, partially removes the rotational constraints on the side chain of Y567. Interestingly, the T587A mutant affects not only the dissociation constant, $K_d$, for the complementary incoming dNTP but also the $k_{pol}$. The double mutant T587A/Y391A has an effect similar to that of the Y567F mutant except that the $k_{pol}$ is not reduced as dramatically. The two changes cited above disrupt the hydrogen bonding network so that the side chain of Y567 is freed from its fixed rotamer position (Figure 1A) and has the potential to rotate like Y567F. Whether the side chain of T587 actually rotates during the reaction cycle, as proposed for D621 and D411 (*36*), remains to be seen. Modeling also suggests that the side chain of T587 may have more freedom to vary its rotamer conformations in the apo-RB69 pol structure than in the ternary complex. A rigid position of this residue in the ternary complex suggests a more direct role for T587 in orienting the nascent base pair for attack by the 3′-OH of the primer terminus (Figures 1A and 6). The observation that the T587A mutant reduces $k_{pol}$ by 4-fold is consistent with this notion and with the extent of $k_{pol}$ reduction which is the same for the T587A/Y391A double mutant. Since the $k_{pol}$ is restored to wild-type levels in the T587A/Y391F double mutant, this suggests that the phenyl ring of Y391 provides a key interaction dictating the side chain rotamer position of T587. It is interesting to note that in the Y391F mutant, there is no reduction in the reaction rate relative to the parental enzyme for incorporation of complementary and noncomplementary dNMPs even though there is a missing hydrogen bond.

In view of the reduced level of base discrimination exhibited by the Y567A mutant, we wondered if this mutant would also be more efficient in its ability to incorporate dFMP, the isosteric analogue of dTMP, as compared to a noncomplementary base such as dGMP. This is an extension of the question about how the loss of steric constraints in the binding pocket, which partially encloses the templating base and incoming dNTP, affects base selection (*37*). Comparison of the parental and Y567A mutant indicates only minor differences between them in their ability to utilize dFTP. The main difference is in the pre-steady-state kinetic parameters, the Y567A mutant having a slightly higher $K_d$ and $k_{pol}$ than the parental enzyme for this substrate. The two opposing values of $K_d$ and $k_{pol}$ effectively offset each other so that the selectivity is only slightly greater (<2-fold) for the Y567A mutant versus the parental enzyme. dFTP has been used in steady-state assays as a probe for the relative importance of geometry versus Watson−Crick hydrogen bonding (*34*). It was shown by Morales and Kool (*33*) to be incorporated more efficiently than mispaired dNTPs but had higher $K_m$ values and lower $k_{cat}$ values than dTTP with both KF and T7 DNA pol. While the studies of Kool and his colleagues have demonstrated the importance of shape, which includes the combined volume of the templating base and the incoming dTTP analogue, they did not underestimate the contribution of Watson−Crick hydrogen bonding in base discrimination (*33*, *37*). Their work did show, however, that as long as geometrical constraints were satisfied, hydrogen bonding was not an absolute requirement for primer extension with this base analogue (*33*). There have not been any reports, to our knowledge, in which dFTP or other dNTP isosteres have been used to obtain pre-steady-state kinetic parameters for DNA polymerases. Our results extend the concept of Morales and Kool (*33*, *37*), showing that the principal effect of the absence of Watson−Crick hydrogen bonding is on $k_{pol}$, presumably due to impaired alignment of the active site residues with the substrates. We cannot tell at present whether the reduction in $k_{pol}$ is due to a slower rate of conformational change or chemistry. Future studies, which will include pre-steady-state burst experiments with dFTP, should allow us to determine if there is a change in the rate-limiting step with this isostere compared to the situation with a complementary dNTP.

## ACKNOWLEDGMENT

We thank Dr. Eric Kool for his generous gift of dFTP, Caroline Kisker for providing us with information about the

Y567F−P/T structure, Karen Anderson for helpful discussions, and Liz Vellali for skillful preparation of the manuscript.

## REFERENCES


1. Franklin, M. C., Wang, J., and Steitz, T. A. (2001) Structure of the replicating complex of a pol alpha family DNA polymerase, *Cell 105*, 657−667.
2. Kornberg, A., and Baker, T. (1992) *DNA Replication*, W. H. Freeman & Co., New York.
3. Schaaper, R. M. (1993) Base selection, proofreading, and mismatch repair during DNA replication in *Escherichia coli*, *J. Biol. Chem. 268*, 23762−23765.
4. Echols, H., and Goodman, M. F. (1991) Fidelity mechanisms in DNA replication, *Annu. Rev. Biochem. 60*, 477−511.
5. Kunkel, T. A., and Bebenek, K. (2000) DNA replication fidelity, *Annu. Rev. Biochem. 69*, 497−529.
6. Goodman, M. F. (2002) Error-prone repair DNA polymerases in prokaryotes and eukaryotes, *Annu. Rev. Biochem. 71*, 17−50.
7. Lehmann, A. (2003) Low-fidelity DNA polymerases, *Curr. Biol. 13*, R585.
8. Parikh, S. S., Mol, C. D., Hosfield, D. J., and Tainer, J. A. (1999) Envisioning the molecular choreography of DNA base excision repair, *Curr. Opin. Struct. Biol. 9*, 37−47.
9. Cleaver, J. E., Collins, C., Ellis, J., and Volik, S. (2003) Genome sequence and splice site analysis of low-fidelity DNA polymerases H and I involved in replication of damaged DNA, *Genomics 82*, 561−570.
10. Scharer, O. D. (2003) Chemistry and biology of DNA repair, *Angew. Chem., Int. Ed. 42*, 2946−2974.
11. Schofield, M. J., and Hsieh, P. (2003) DNA mismatch repair: Molecular mechanisms and biological function, *Annu. Rev. Microbiol. 57*, 579−608.
12. McGowan, C. H. (2003) Running into problems: How cells cope with replicating damaged DNA, *Mutat. Res. 532*, 75−84.
13. Stivers, J. T., and Jiang, Y. L. (2003) A mechanistic perspective on the chemistry of DNA repair glycosylases, *Chem. Rev. 103*, 2729−2759.
14. Friedberg, E. C. (2003) DNA damage and repair, *Nature 421*, 436−440.
15. Johnson, S. J., and Beese, L. S. (2004) Structures of mismatch replication errors observed in a DNA polymerase, *Cell 116*, 803−816.
16. Braithwaite, D. K., and Ito, J. (1993) Compilation, alignment, and phylogenetic relationships of DNA polymerases, *Nucleic Acids Res. 21*, 787−802.
17. Hubscher, U., Maga, G., and Spadari, S. (2002) Eukaryotic DNA polymerases, *Annu. Rev. Biochem. 71*, 133−163.
18. Wang, J., Sattar, A. K., Wang, C. C., Karam, J. D., Konigsberg, W. H., and Steitz, T. A. (1997) Crystal structure of a pol alpha family replication DNA polymerase from bacteriophage RB69, *Cell 89*, 1087−1099.
19. Capson, T. L., Peliska, J. A., Kaboord, B. F., Frey, M. W., Lively, C., Dahlberg, M., and Benkovic, S. J. (1992) Kinetic characterization of the polymerase and exonuclease activities of the gene 43 protein of bacteriophage T4, *Biochemistry 31*, 10984−10994.
20. Joyce, C. M., and Steitz, T. A. (1994) Function and structure relationships in DNA polymerases, *Annu. Rev. Biochem. 63*, 777−822.
21. Steitz, T. A. (1999) DNA polymerases: Structural diversity and common mechanisms, *J. Biol. Chem. 274*, 17395−17398.
22. Reha-Krantz, L. J. (1995) Learning about DNA polymerase function by studying antimutator DNA polymerases, *Trends Biochem. Sci. 20*, 136−140.
23. Shamoo, Y., and Steitz, T. A. (1999) Building a replisome from interacting pieces: Sliding clamp complexed to a peptide from DNA polymerase and a polymerase editing complex, *Cell 99*, 155−166.
24. Karam, J. D., and Konigsberg, W. H. (2000) DNA polymerase of the T4-related bacteriophages, *Prog. Nucleic Acid Res. Mol. Biol. 64*, 65−96.
25. Yang, G., Franklin, M., Li, J., Lin, T. C., and Konigsberg, W. (2002) A conserved Tyr residue is required for sugar selectivity in a Pol alpha DNA polymerase, *Biochemistry 41*, 10256−10261.
26. Yeh, L. S., Hsu, T., and Karam, J. D. (1998) Divergence of a DNA replication gene cluster in the T4-related bacteriophage RB69, *J. Bacteriol. 180*, 2005−2013.
27. Spacciapoli, P., and Nossal, N. G. (1994) Interaction of DNA polymerase and DNA helicase within the bacteriophage T4 DNA replication complex. Leading strand synthesis by the T4 DNA polymerase mutant A737V (tsL141) requires the T4 gene 59 helicase assembly protein, *J. Biol. Chem. 269*, 447−455.
28. Wu, P., Nossal, N., and Benkovic, S. J. (1998) Kinetic characterization of a bacteriophage T4 antimutator DNA polymerase, *Biochemistry 37*, 14748−14755.
29. Yang, G., Lin, T., Karam, J., and Konigsberg, W. H. (1999) Steady-state kinetic characterization of RB69 DNA polymerase mutants that affect dNTP incorporation, *Biochemistry 38*, 8094−8101.
30. Abdus Sattar, A. K., Lin, T. C., Jones, C., and Konigsberg, W. H. (1996) Functional consequences and exonuclease kinetic parameters of point mutations in bacteriophage T4 DNA polymerase, *Biochemistry 35*, 16621−16629.
31. Yang, G., Franklin, M., Li, J., Lin, T. C., and Konigsberg, W. (2002) Correlation of the kinetics of finger domain mutants in RB69 DNA polymerase with its structure, *Biochemistry 41*, 2526−2534.
32. Liu, D., Moran, S., and Kool, E. T. (1997) Bi-stranded, multisite replication of a base pair between difluorotoluene and adenine: Confirmation by 'inverse' sequencing, *Chem. Biol. 4*, 919−926.
33. Morales, J. C., and Kool, E. T. (2000) Functional hydrogen-bonding map of the minor groove binding tracks of six DNA polymerases, *Biochemistry 39*, 12979−12988.
34. Bebenek, A., Dressman, H. K., Carver, G. T., Ng, S., Petrov, V., Yang, G., Konigsberg, W. H., Karam, J. D., and Drake, J. W. (2001) Interacting fidelity defects in the replicative DNA polymerase of bacteriophage RB69, *J. Biol. Chem. 276*, 10387−10397.
35. Skelly, J. V., Edwards, K. J., Jenkins, T. C., and Neidle, S. (1993) Crystal structure of an oligonucleotide duplex containing G·G base pairs: Influence of mispairing on DNA backbone conformation, *Proc. Natl. Acad. Sci. U.S.A. 90*, 804−808.
36. Zakharova, E., Wang, J., and Konigsberg, W. (2004) The Activity of Selected RB69 DNA Polymerase Mutants Can Be Restored by Manganese Ions: The Existence of Alternative Metal Ion Ligands Used during the Polymerization Cycle, *Biochemistry 43*, 6587−6595.
37. Kool, E. T. (2002) Active site tightness and substrate fit in DNA replication, *Annu. Rev. Biochem. 71*, 191−219.


BI047921X